Supplementary Information

Device Physics of Back-Contact Perovskite Solar Cells

Zhenhai Yang,[ab] Weichuang Yang,[a] Xi Yang,[a] James Greer,[*b] Jiang Sheng,[*a] Baojie Yan[a] and Jichun Ye[*a]

[a]Ningbo Institute of Materials Technology and Engineering, Chinese Academy of Sciences (CAS), Ningbo 315201, China. E-mail: shengjiang@nimte.ac.cn; jichun.ye@nimte.ac.cn

[b]Department of Electrical and Electronic Engineering, Faculty of Science and Engineering, The University of Nottingham, Ningbo 315100, China. E-mail: Jim.Greer@nottingham.edu.cn

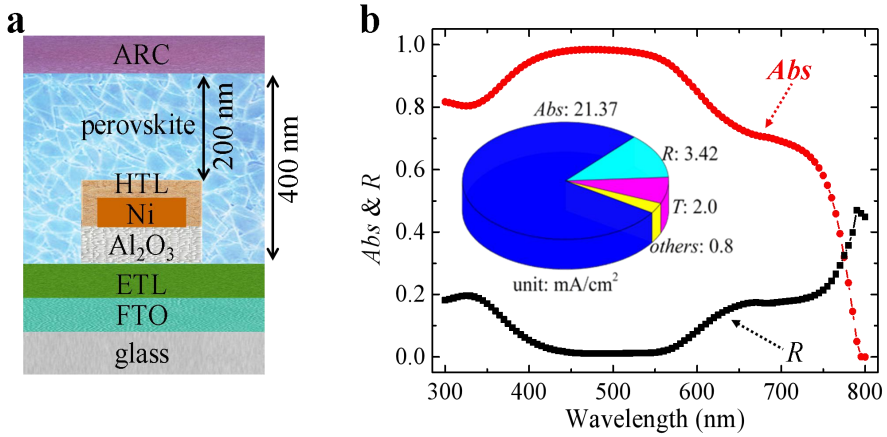

Fig. S1 (a) Schematic of QIBC PSCs with the effective perovskite of 300 nm. (b) *Abs* and *R* spectra of QIBC PSCs. The inserted pie graph is the distribution of the corresponding current densities.

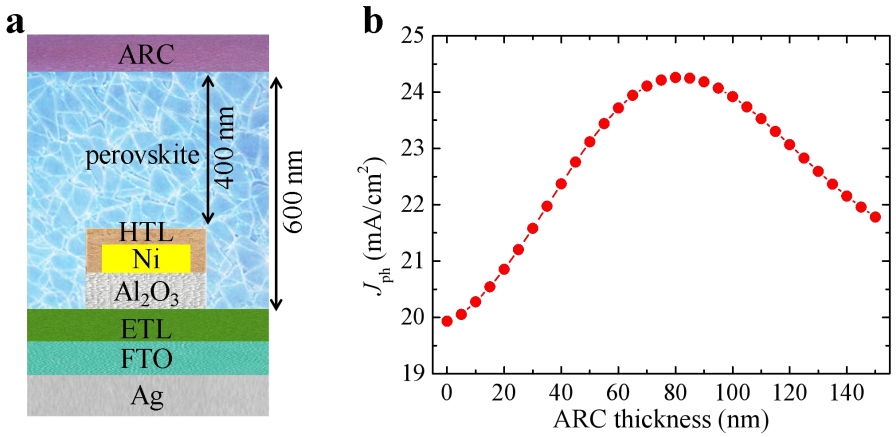

Fig. S2 (a) Schematic of QIBC PSCs with the effective perovskite of 500 nm. (b) J_{ph} as a function of ARC thickness.

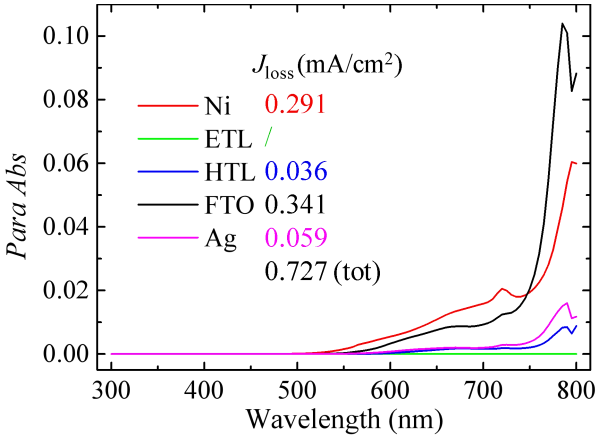

Fig. S3 *Para Abs* spectra of QIBC PSCs with the corresponding current-density loss (J_{loss}) inserted in the figure.

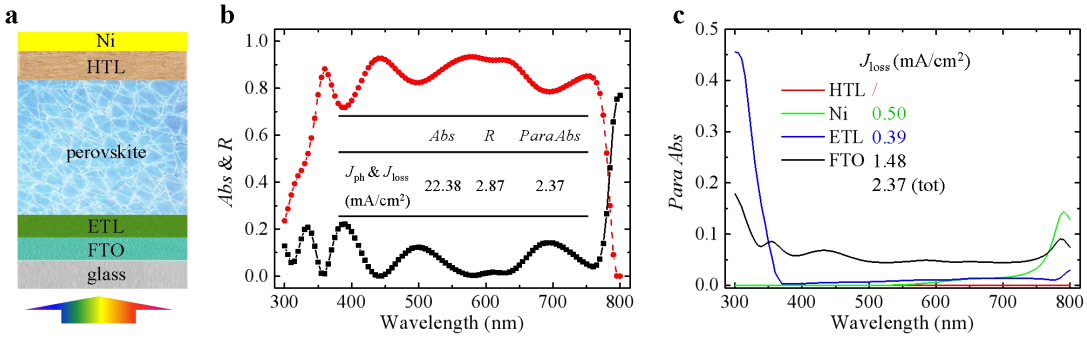

Fig. S4 (a) Schematic of sandwich PSCs with the effective perovskite of 500 nm. (b) *Abs* and *R* spectra of sandwich PSCs. (c) *Para Abs* spectra of sandwich PSCs with the corresponding J_{loss} inserted in the figure.

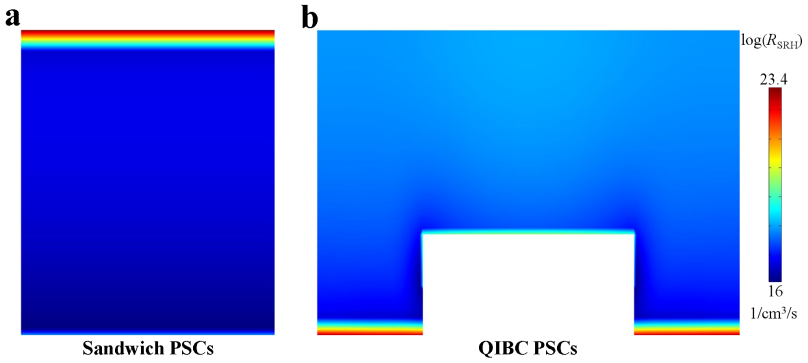

Fig. S5 Recombination loss distributions within perovskite regions for (a) sandwich and (b) QIBC PSCs under $D_{it\_ETL} = 10^{13}$ cm^{-2} at the MP condition.

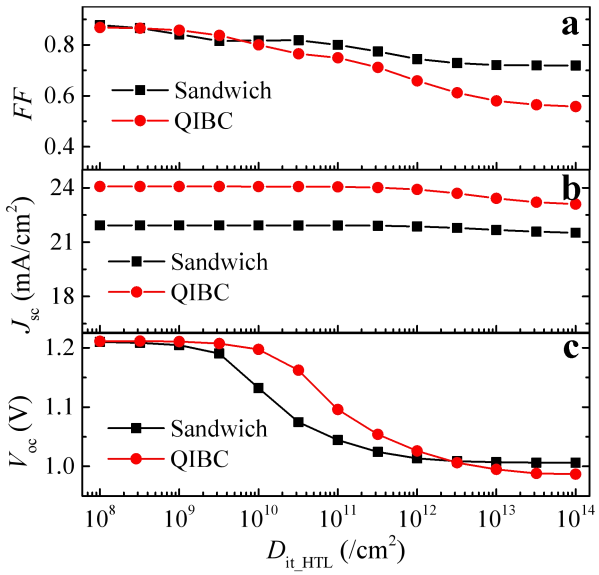

Fig. S6 Dependence of (a) *FF*, (b) J_{sc} and (c) V_{oc} of QIBC and sandwich PSCs on D_{it_HTL}.

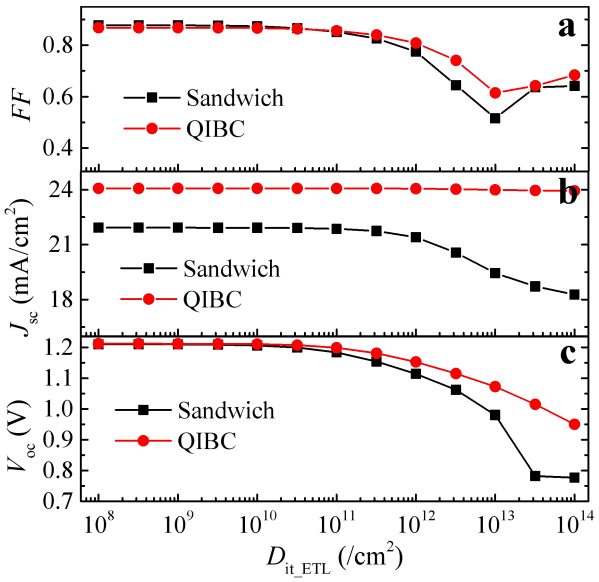

Fig. S7 Dependence of (a) *FF*, (b) J_{sc} and (c) V_{oc} of QIBC and sandwich PSCs on D_{it_ETL}.

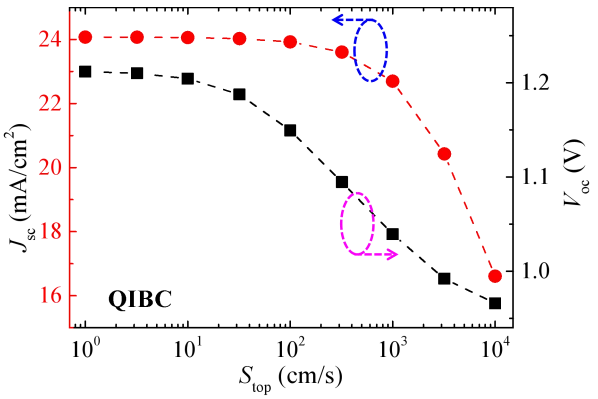

Fig. S8 Dependence of J_{sc} and V_{oc} of QIBC PSCs on S_{top}.

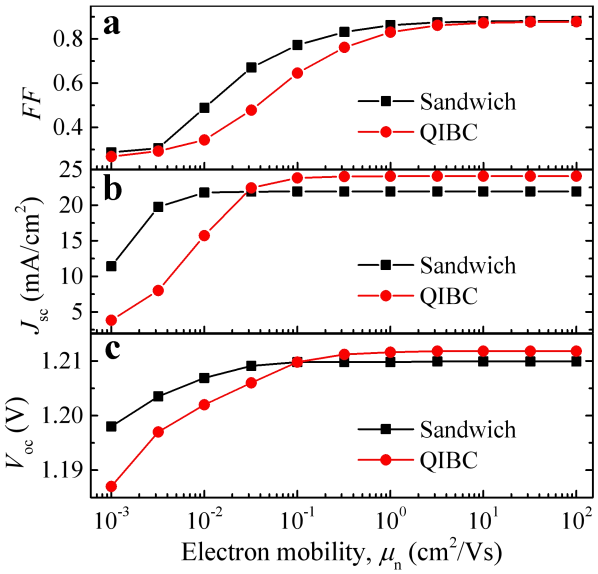

Fig. S9 Dependence of (a) *FF*, (b) J_{sc} and (c) V_{oc} of QIBC and sandwich PSCs on μ_n of perovskite.

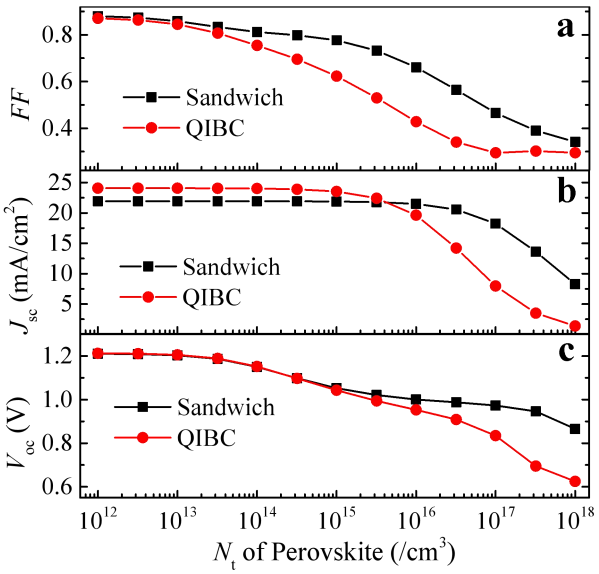

Fig. S10 Dependence of (a) *FF*, (b) J_{sc} and (c) V_{oc} of QIBC and sandwich PSCs on N_t of perovskite.

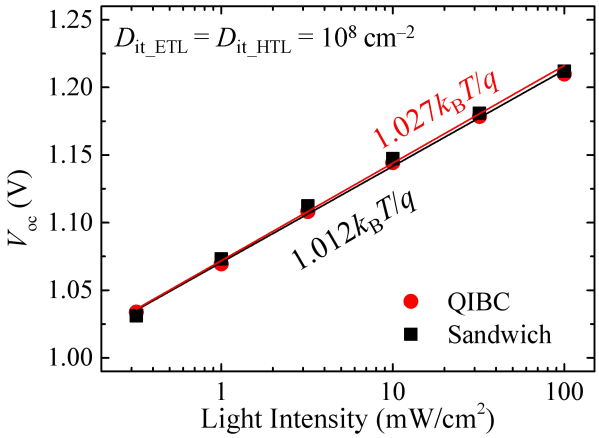

Fig. S11 V_{oc} versus light intensity for QIBC and sandwich PSCs under $D_{it\_HTL} = D_{it\_ETL} = 10^8$ cm^{-2}.

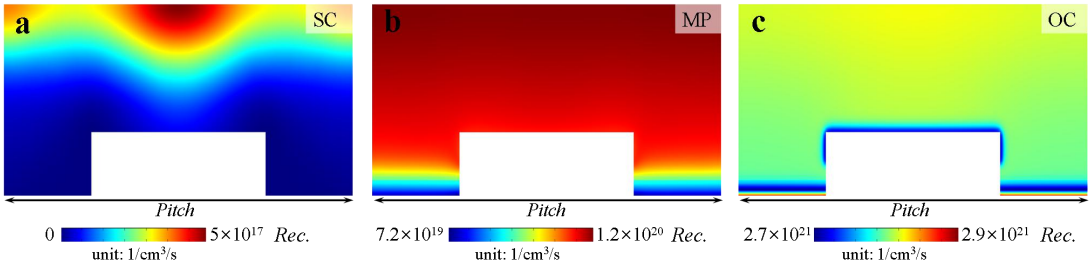

Fig. S12 Recombination loss distribution within perovskite regions under (a) SC, (b) MP and (c) OC conditions.

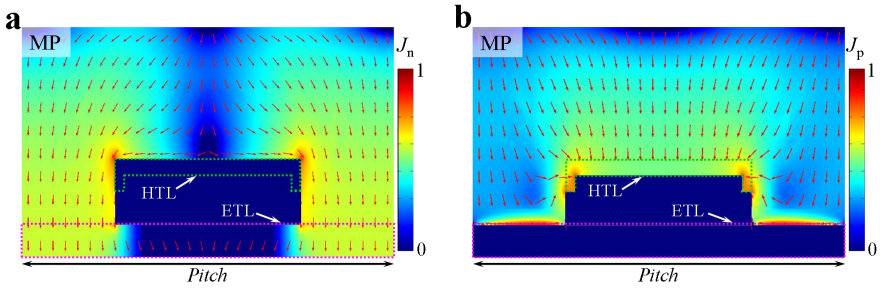

Fig. S13 (a) J_n and (b) J_p distributions within perovskite, ETL and HTL regions under the MP condition, where the red arrows represent the current density direction.

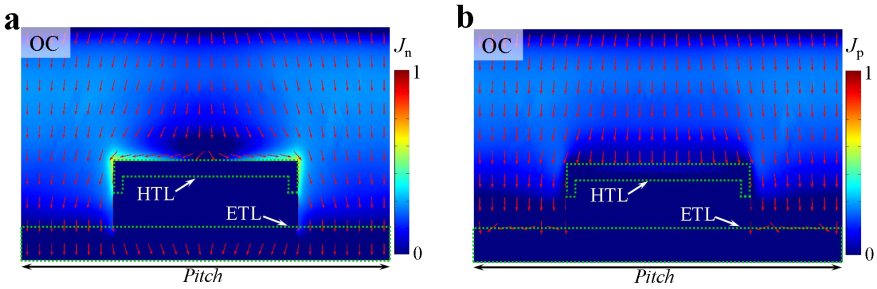

Fig. S14 (a) J_n and (b) J_p distribution within perovskite, ETL and HTL regions under the OC condition, where the red arrows represent the current density direction.

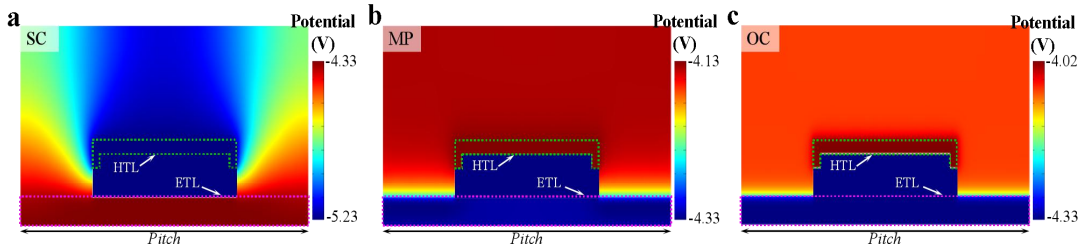

Fig. S15 2D cross-sectional potential distribution under (a) SC, (b) MP and (c) OC conditions.

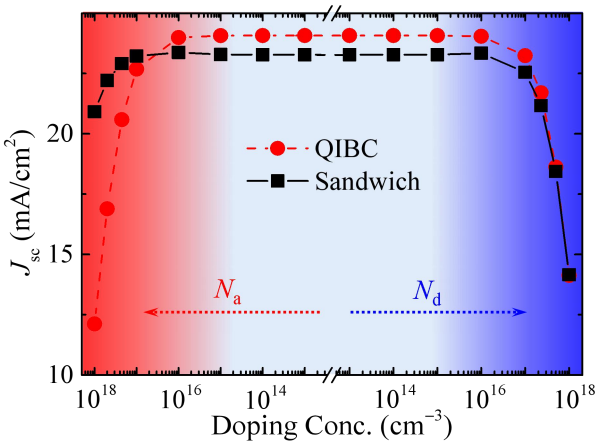

Fig. S16 J_{sc} of QIBC and Sandwich PSCs as a function of perovskite doping concentration.

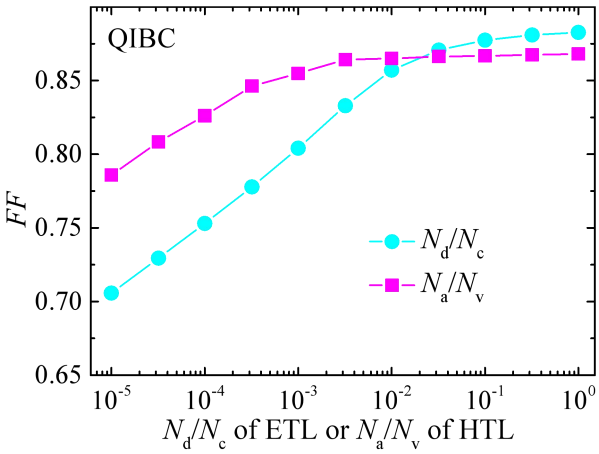

Fig. S17 *FF* of QIBC PSCs under various N_d/N_c of ETL and N_a/N_v of HTL.

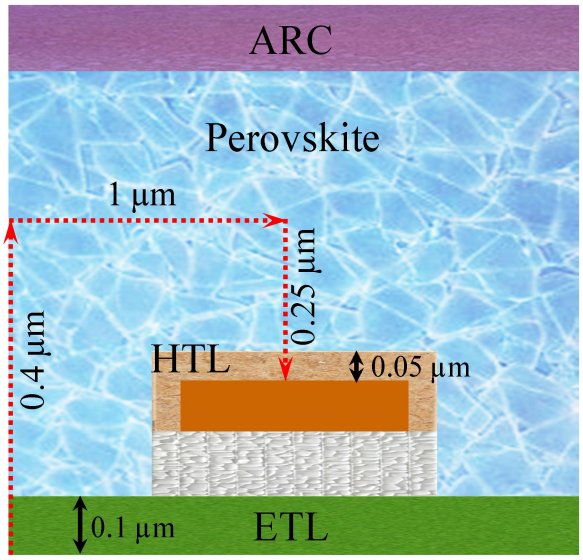

Fig. S18 Position intercepting inside the perovskite film for the QIBC structure.

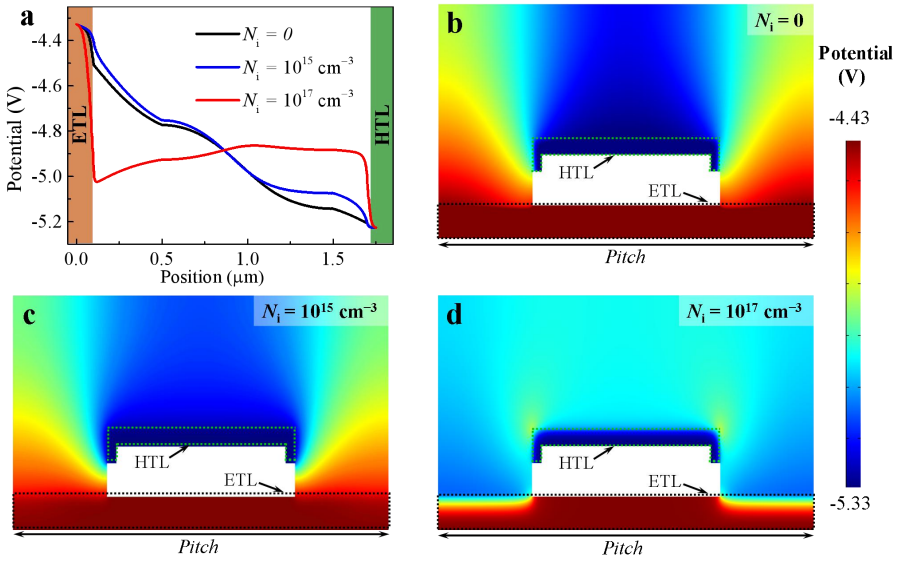

Fig. S19 Linear and 2D cross-sectional potential distribution under N_i = 0, 10^{15} and 10^{17} cm^{-3}.

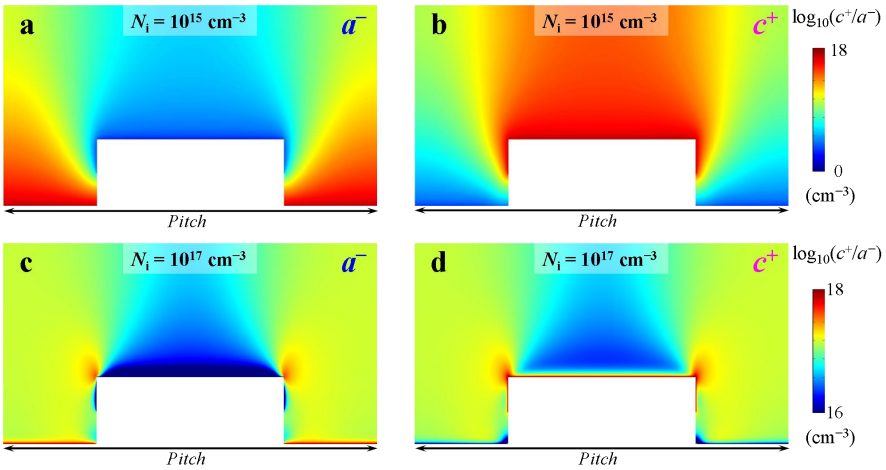

Fig. S20 Concentration distribution of anions and cations within perovskite region under N_i = 10^{15} and 10^{17} cm^{-3}.

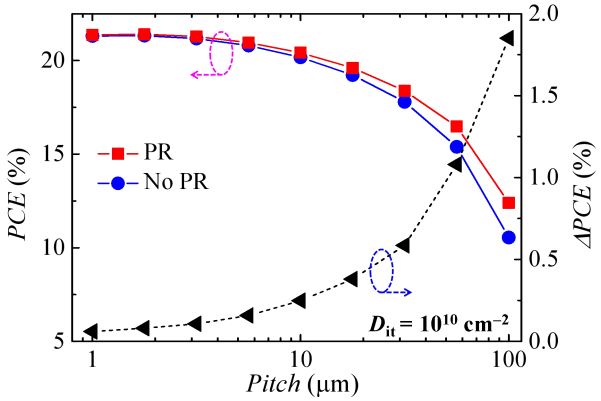

Fig. S21 *PCE* and Δ*PCE* of QIBC PSCs as a function of *Pitch* under *ff* = 0.5 with D_{it} =10^{10} cm^{-2} for no-PR and PR cases.

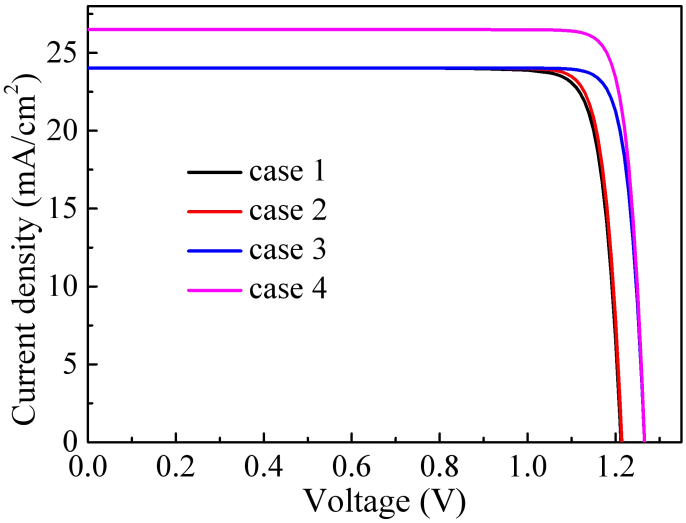

Fig. S22 *J-V* curves of QIBC PSCs under different cases.

Table S1 Parameters used for simulation.[1-4]

Material parameters	ETL	Perovskite	HTL
Thickness, nm	100	400-600	50
Electron affinity, χ (eV)	4.23	3.93	1.7
Bandgap energy, E_g (eV)	3.7	1.55	3.6
Relative dielectric permittivity, ε	9	6.5	12
Effective conduction band density, N_c (cm^{-3})	4.36×10^{18}	2.8×10^{18}	9.15×10^{17}
Effective valence band density, N_v (cm^{-3})	2.52×10^{19}	1.8×10^{19}	4.54×10^{18}
Donor doping concentration, N_d (cm^{-3})	1×10^{17}	/	/
Acceptor doping concentration, N_a (cm^{-3})	/	1×10^{13}	2.66×10^{17}
Mobility of electron/hole, μ_n/μ_p (cm^2/Vs)	$1.9\times10^{-3}/1.9\times10^{-3}$	12.5/7.5	0.01/0.01
SRH life time, τ_n/τ_p (s)	0.083/0.083	$2.73\times10^{-6}/2.73\times10^{-6}$	$1\times10^{-6}/1\times10^{-6}$
Radiative recombination coefficient, B_{rad} (cm^3s^{-1})	/	3.27×10^{-11}	/
Auger recombination coefficient, A_n/A_p (cm^6s^{-1})	/	0.88×10^{-29}	/
Acceptor doping concentration, N_a, cm^{-3}	/	1×10^{20}	/

Table S2 Simulated *PCE* for different ETL/HTL designs.

ETL/HTL designs	CBO (eV)	VBO (eV)	*PCE* (%)
PCBM/CuO or PCBM/Cu_2O	-0.37	-0.08	24.71
TiO_2/Cu_2O	-0.07	-0.08	25.50
ZnO/NiO_x	-0.47	-0.18	22.95
PCBM/NiO_x	-0.37	-0.18	24.69
SnO_2/NiO_x	-0.30	-0.18	25.32
TiO_2/NiO_x	-0.07	-0.18	25.47
ZnO/Spiro-MeOTAD	-0.47	-0.28	22.93
TiO_2/Spiro-MeOTAD or TiO_2/CuI	-0.07	-0.28	25.40
ZnO/PEDOT:PSS	-0.47	-0.38	22.65
SnO_2/Spiro-MeOTAD	-0.30	-0.28	25.30
ZnO/P3HT	-0.47	-0.48	21.45
TiO_2/P3HT	-0.07	-0.48	23.44
IBCA/P3HT	0.23	-0.48	21.97

References

1. Y. An, A. Shang, G. Cao, S. Wu, D. Ma and X. Li, *Solar RRL*, 2018, **2**, 1800126.
2. Y. Da, Y. Xuan and Q. Li, *Sol. Energ. Mater. Sol. C*, 2018, **174**, 206–213.
3. P. Zhao, Z. Lin, J. Wang, M. Yue, J. Su, J. Zhang, J. Chang and Y. Hao, *ACS Appl. Energy Mater.*, 2019, **2**, 4504–4512.
4. X. Wei, X. Wang, H. Jiang, Y. Huang, A. Han, Q. Gao, J. Bian and Z. Liu, *Superlattice Microst.*, 2017, **112**, 383–393.